

Analysis of the Principles Governing Proton-Transfer Reactions. Comparison of the Imine and Amine Groups

Eric A. Hillenbrand and Steve Scheiner*†

Contribution from the Department of Chemistry and Biochemistry, Southern Illinois University, Carbondale, Illinois 62901. Received May 28, 1985

Abstract: Proton transfers involving the imine and amine groups are studied by ab initio SCF calculations with use of the 4-31G* basis set with $\text{H}_2\text{C}=\text{NH}$ and NH_3 serving as respective models of the two groups. The potential energy surface of the imine- H^+ -amine system contains two distinct minima, corresponding to $(\text{H}_2\text{CHNH}-\text{NH}_3)^+$ and $(\text{H}_2\text{CHN}-\text{HNH}_3)^+$, the former being the more stable, separated by a barrier of 5.9 kcal/mol. The energy barrier separating the two minima rises rapidly as the H bond is elongated; nevertheless, the $(\text{H}_2\text{CHNH}-\text{NH}_3)^+$ configuration remains the more stable regardless of the H bond length. On the other hand, the relative energies of the two minima are profoundly affected by angular distortions of the bond. In general, rotation of either subunit, turning its N lone pair away from the N--N axis, causes a preferential stabilization of the configuration in which the proton is associated with that group, an effect attributed to a more favorable ion-dipole interaction. An exception to this rule is noted with distortions out of the imine plane; the differing behavior of the amine and imine groups is traced to the opposite sign of the appropriate components of their quadrupole moments. These same principles explain the results obtained for the oxygen analogues carbonyl and hydroxyl after consideration of the additional factor that the dipole moment vectors of these groups do not coincide with the directions of the O lone pairs.

Renewed interest has been focused on the proton-transfer process with the recent development of experimental techniques¹⁻⁸ capable of studying the process in the gas phase, free of complicating solvent effects. Although these methods have provided a great deal of valuable insight into the essential features of the process, they suffer from a number of limitations. Ab initio molecular orbital techniques are capable of supplementing the experimental data by facilitating study of transient species and determination of detailed molecular geometries.

Recent calculations in this laboratory⁹⁻¹⁷ have demonstrated the sensitivity of the energetics of the proton-transfer process to the precise geometry of the H bond. A detailed comparison of proton transfers involving H_2CO and HOH pointed out a number of important differences in behavior between the doubly-bonded oxygen present in the carbonyl group and the single bonds of the hydroxyl.^{17b} Along parallel lines, it would be interesting to extend the investigation to nitrogen atoms which are also frequently involved in H bonding. The present study therefore consists of a comparison of proton transfers involving the $\text{C}=\text{N}$ group of imines with the singly-bonded N in amines. We select as our model imine H_2CNH , the N analogue of H_2CO , while NH_3 serves as our prototype amine. Proton transfers between these two molecules are examined in the $(\text{H}_2\text{CHN}-\text{H}-\text{NH}_3)^+$ complex; data computed for $(\text{H}_3\text{N}-\text{H}-\text{NH}_3)^+$ allow a direct comparison of the imine and amine functions with regard to proton transfers.

A particularly intriguing finding of the previous work¹⁷ was the possibility that a proton can be shifted from the carbonyl group to the hydroxyl merely by angular reorientations of the two groups relative to one another. Specifically, since the proton affinity of H_2CO is greater than that of H_2O , it is not surprising that $(\text{H}_2\text{COH}-\text{OH}_2)^+$ is more stable than $(\text{H}_2\text{CO}-\text{HOH}_2)^+$. However, this order of stability is reversed when the hydroxyl group lies along the $\text{C}=\text{O}$ axis of H_2CO rather than along a carbonyl lone pair direction. A similar observation in the nitrogen analogues would be of especial importance to understanding the mechanism by which bacteriorhodopsin pumps protons across its biomembrane since the protonation/deprotonation of the imine group of the Schiff base chromophore is known to play a primary role in the functioning of this protein.¹⁸⁻²¹

After describing the theoretical method used and the reason for its choice, this procedure is applied first to examination of the potential energy surfaces of the $(\text{H}_2\text{CHN}-\text{H}-\text{NH}_3)^+$ and $(\text{H}_3\text{N}-\text{H}-\text{NH}_3)^+$ complexes in the gas phase, free of any geometrical constraints. The succeeding sections treat these systems as models of H bonds involving imine and amine groups within a single large

molecule and therefore consider the various bond lengths and angles likely to be observed within such intramolecular H bonds. Comparisons are drawn with the previous calculations involving the oxygen analogues throughout so as to elucidate the principles governing the general proton transfer reaction and thereby provide chemists with a basis for understanding this process and predicting the energetics and kinetics in any system from first principles.

- (1) Moylan, C. R.; Brauman, J. I. *Annu. Rev. Phys. Chem.* **1983**, *34*, 187.
- (2) Moylan, C. R.; Brauman, J. I. *J. Phys. Chem.* **1984**, *88*, 3175.
- (3) Ausloos, P.; Lias, S. G. *J. Am. Chem. Soc.* **1981**, *103*, 3641. Lias, S. G. *J. Phys. Chem.* **1984**, *88*, 4401.
- (4) Squires, R. R.; Bierbaum, V. M.; Grabowski, J. J.; DePuy, C. H. *J. Am. Chem. Soc.* **1983**, *105*, 5185.
- (5) Bohme, D. K.; Rakshit, A. B.; Mackay, G. I. *J. Am. Chem. Soc.* **1982**, *104*, 1100.
- (6) Meot-Ner, M. *J. Am. Chem. Soc.* **1984**, *106*, 1257.
- (7) Rossetti, R.; Rayford, R.; Haddon, R. C.; Brus, L. E. *J. Am. Chem. Soc.* **1981**, *103*, 4303.
- (8) Van Benthem, M. H.; Gillispie, G. D. *J. Phys. Chem.* **1984**, *88*, 2954.
- (9) Bowers, M. T., Ed. "Gas Phase Ion Chemistry"; Academic Press: New York, 1979.
- (10) Scheiner, S. *Acc. Chem. Res.* **1985**, *18*, 174.
- (11) Scheiner, S. *J. Am. Chem. Soc.* **1981**, *103*, 315. Scheiner, S. *Ann. N.Y. Acad. Sci.* **1981**, *367*, 493.
- (12) Scheiner, S. *J. Phys. Chem.* **1982**, *86*, 376.
- (13) Scheiner, S. *J. Chem. Phys.* **1982**, *77*, 4039; **1984**, *80*, 1982. Scheiner, S.; Bigham, L. D. *Ibid.* **1985**, *82*, 3316.
- (14) Hillenbrand, E. A.; Scheiner, S. *J. Am. Chem. Soc.* **1984**, *106*, 6266.
- (15) Scheiner, S.; Redfern, P.; Szczesniak, M. M. *J. Phys. Chem.* **1985**, *89*, 262. Szczesniak, M. M.; Scheiner, S. *Ibid.* **1985**, *89*, 1835.
- (16) Szczesniak, M. M.; Scheiner, S. *J. Chem. Phys.* **1982**, *77*, 4586. Scheiner, S.; Szczesniak, M. M.; Bigham, L. D. *Int. J. Quantum Chem.* **1983**, *23*, 739.
- (17) (a) Scheiner, S.; Harding, L. B. *J. Am. Chem. Soc.* **1981**, *103*, 2169. Scheiner, S.; Harding, L. B. *Chem. Phys. Lett.* **1981**, *79*, 39. Scheiner, S.; Harding, L. B. *J. Phys. Chem.* **1983**, *87*, 1145.
- (18) (a) Scheiner, S.; Hillenbrand, E. A. *Proc. Natl. Acad. Sci. U.S.A.* **1985**, *82*, 2741. (b) Scheiner, S.; Hillenbrand, E. A. *J. Phys. Chem.* **1985**, *89*, 3053.
- (19) Lewis, A.; Marcus, M. A.; Ehrenberg, B.; Crespi, H. *Proc. Natl. Acad. Sci. U.S.A.* **1978**, *75*, 4642. Lewis, A. *Methods Enzymol.* **1982**, *88*, 561.
- (20) Konishi, T.; Tristram, S.; Packer, L. *Photochem. Photobiol.* **1979**, *29*, 353. Konishi, T.; Packer, L. *FEBS Lett.* **1978**, *92*, 1.
- (21) Bayley, H.; Radhakrishnan, R.; Huang, K.-S.; Khorana, H. G. *J. Biol. Chem.* **1981**, *256*, 3797.
- (22) Smith, S. O.; Myers, A. B.; Pardo, J. A.; Winkel, C.; Mulder, P. P. J.; Lugtenberg, J.; Mathies, R. *Proc. Natl. Acad. Sci. U.S.A.* **1984**, *81*, 2055.

* Recipient of an NIH Research Career Development Award (1982-1987).

Methods

All calculations described herein were carried out with the ab initio GAUSSIAN-80 set of computer programs.²² A primary reason for selection of the 4-31G* basis set²³ in our previous study of H₂CO and H₂O was its accurate reproduction of the experimentally determined difference in proton affinity between these two molecules. The situation is less clearly defined in the nitrogen case since it has not been possible to accurately measure the proton affinity of H₂CNH to date. Fortunately, ab initio calculations have been carried out previously at rather high levels of theory for both H₂CNH and NH₃. Using fourth-order Møller–Plesset perturbation theory in conjunction with a 6-31G** basis set, Del Bene et al.²⁴ found the electronic contribution to the proton affinities of these two molecules to be 225.3 and 220.8 kcal/mol, respectively, a difference of 4.5 kcal/mol. The corresponding values at the SCF level using the 4-31G* basis set are 223.5 and 218.2 kcal/mol, rather close to the more reliable values above. Perhaps more important, the SCF/4-31G* proton affinity of H₂CNH is 5.3 kcal/mol higher than that of NH₃, in excellent agreement with the most reliable calculations to date.²⁴ Moreover, after appropriate modifications for zero-point vibrational energy and thermal corrections,²⁴ the above proton-affinity difference is within the range of uncertainty of the experimental measurements.²⁵

In addition to its adequate treatment of the relative proton affinities of the two molecules in question, the split-valence characteristic and presence of d orbitals in 4-31G* should provide sufficient flexibility for electronic rearrangements occurring during the proton transfer. Our prior calculations^{9–16} have led to the conclusion that transfer barriers increase with enlarged basis sets. Augmentation of our basis with additional valence or polarization functions would therefore produce significantly higher barriers. However, since inclusion of correlation has been found to lower the barrier, some degree of cancellation between these two effects is expected. While we cannot presume this cancellation to be complete, we do not think our computed barriers will be in error by more than perhaps 2 or 3 kcal/mol. In any event, it is clear that the qualitative trends, which represent the major thrust of this work, will be accurately reproduced with the 4-31G* basis set at the SCF level. Finally, use of this basis set will facilitate direct comparison with our previous calculations of the oxygen analogues.^{17b}

Full Optimizations

We begin our study of the (H₂CHN–H–NH₃)⁺ system with a full optimization of its geometry, illustrated in Figure 1. α refers to the angle between the C=N bond and the N–N axis. The only assumption made about the geometry of the complex is that the NH₃ subunit maintains a local C₃ symmetry axis in the complex, indicated by the dotted line in Figure 1. The angle made by this line with the N–N axis is designated as β . The deviation of the central proton H^c from the N–N axis is represented by δ , assigned a positive value when H^c lies below the axis. The imine group was found to prefer a planar geometry for all configurations considered below. A full geometry optimization of the (H₃N–H–NH₃)⁺ complex led to a C_{3v} structure in which each NH₃ subunit contains a local C₃ symmetry axis. The central proton lies along the N–N axis which is collinear with the C₃ axes of the two subunits which are in turn staggered with respect to one another. The transition state to proton transfer in which the proton is midway between the two N atoms belongs to the D_{3d} point group. The threefold symmetry of each subunit was maintained in the angularly distorted H bonds described below.

(22) Binkley, J. S.; Whiteside, R. A.; Krishnan, R.; Seeger, R.; DeFrees, D. J.; Schlegel, H. B.; Topiol, S.; Kahn, L. R.; Pople, J. A. *QCPE* 1981, No. 406.

(23) Ditchfield, R.; Hehre, W. J.; Pople, J. A. *J. Chem. Phys.* 1971, 54, 724. Hehre, W. J.; Ditchfield, R.; Pople, J. A. *Ibid.* 1972, 56, 2257. Collins, J. B.; Schleyer, P. v. R.; Binkley, J. S.; Pople, J. A. *Ibid.* 1976, 64, 5142.

(24) Del Bene, J. E.; Frisch, M. J.; Raghavachari, K.; Pople, J. A. *J. Phys. Chem.* 1982, 86, 1529.

(25) Wolf, J. F.; Staley, R. H.; Koppel, I.; Taagepera, M.; McIver, R. J., Jr.; Beauchamp, J. L.; Taft, R. W. *J. Am. Chem. Soc.* 1977, 99, 5417.

Table 1. Optimized Geometries of (H₂CHN–H–NH₃)⁺ and Isolated Subsystems (All Distances Are in Å and Angles in Degrees)^a

| | R(NIN) | r(N ^a H ^c) | r(CN ^b) | r(N ^a H _N) | r(CH ₁) | r(CH ₂) | r(N ^b H) | δ | α | β | θ (H ₁ CN ^a) | θ (H ₂ CN ^a) | θ (CN ^a H _N) | θ (HN ^b H) | E _i kcal/mol |
|---|--------|-----------------------------------|---------------------|-----------------------------------|---------------------|---------------------|---------------------|----------|----------|---------|--|--|--|------------------------------|----------------------------|
| (H ₂ CNH ₂) ⁺ + NH ₃ | | 1.006 | 1.261 | 1.006 | 1.074 | 1.074 | 1.003 | | | | 119.8 | 119.8 | 121.9 | 107.0 | 24.5 |
| (H ₂ CHNH–NH ₃) ⁺ | 2.823 | 1.047 | 1.256 | 1.004 | 1.074 | 1.074 | 1.006 | –0.2 | 122.0 | 2.3 | 120.8 | 119.4 | 120.7 | 106.1 | 0.0 ^b |
| (H ₂ CHN–H–NH ₃) ⁺ | 2.582 | 1.320 | 1.254 | 1.005 | 1.076 | 1.076 | 1.008 | –0.5 | 125.2 | 1.6 | 122.4 | 119.8 | 115.7 | 107.6 | 5.9 |
| (H ₂ CHN–H–NH ₃) ⁺ | 2.788 | 1.725 | 1.253 | 1.006 | 1.078 | 1.077 | 1.010 | –0.6 | 129.4 | 1.0 | 123.3 | 119.9 | 112.6 | 108.9 | 2.8 |
| H ₂ CNH + (NH ₄) ⁺ | | | 1.247 | 1.006 | 1.084 | 1.079 | 1.014 | | | | 124.7 | 119.3 | 111.7 | 109.5 | 29.7 |

^a See Figure 1 for definition of parameters. ^b E_{SCF} = –150.46104 au.

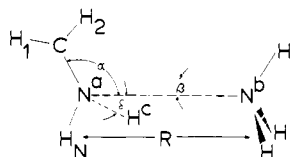


Figure 1. Geometry of $(\text{H}_2\text{CHN}-\text{H}-\text{NH}_3)^+$. Local C_{3v} symmetry was assumed for the NH_3 subunit; the C_3 rotation axis is designated by the dotted line. R refers to the internuclear distance.

The geometrical parameters of the fully optimized complex are contained in the second row of Table I. This structure is designated $(\text{H}_2\text{CHNH}-\text{NH}_3)^+$ since the central proton H^c lies much closer to N^a (1.047 Å) than to N^b (1.776 Å). The binding energy of this complex, relative to the isolated subunits $(\text{H}_2\text{CNH}_2)^+$ and NH_3 , is 24.5 kcal/mol, as indicated by the last entry in the first row of Table I. In addition to $(\text{H}_2\text{CHNH}-\text{NH}_3)^+$, a second minimum is located on the potential energy hypersurface, corresponding to $(\text{H}_2\text{CHN}-\text{HNH}_3)^+$, in which the central proton is more closely associated with the NH_3 subunit. As may be seen by the fourth row of Table I, this configuration is 2.8 kcal/mol higher in energy than $(\text{H}_2\text{CHNH}-\text{NH}_3)^+$. The transition state separating these two minima was located and its geometry is listed in row 3. This structure may be seen to lie 5.9 kcal/mol higher in energy than $(\text{H}_2\text{CHNH}-\text{NH}_3)^+$ and is 3.1 kcal/mol less stable than the other minimum. Following proton transfer, dissociation of $(\text{H}_2\text{CHN}-\text{HNH}_3)^+$ to H_2CNH and $(\text{NH}_4)^+$ requires 26.9 kcal/mol.

In contrast, the surface of $(\text{H}_3\text{N}-\text{H}-\text{NH}_3)^+$ is completely symmetric. The two equivalent minima $(\text{H}_3\text{N}-\text{NH}_3)^+$ and $(\text{H}_3\text{N}-\text{HNH}_3)^+$ are separated by an energy barrier of 3.9 kcal/mol. Dissociation of the complex to $(\text{NH}_4)^+$ and NH_3 is endothermic by 27.2 kcal/mol. It is noted that the data reported here follow a pattern of bracketing as follows. Let us designate the symmetric $(\text{H}_3\text{N}-\text{H}-\text{NH}_3)^+$ system as $(\text{A}-\text{H}-\text{A})^+$ and then replace the left subunit by a group of higher proton affinity B (H_2CNH). The dissociation energy of the $(\text{BH}-\text{A})^+$ complex to BH^+ and A is diminished by the replacement while the dissociation to $\text{B} + \text{AH}^+$ is increased. These dissociation energies of 24.5 and 29.7 kcal/mol bracket the value for $(\text{AH}-\text{A})^+$ of 27.2 kcal/mol. A like pattern was noted in the oxygen case where the left-hand H_2O of $(\text{H}_2\text{O}-\text{H}-\text{OH}_2)^+$ was replaced by the more basic H_2CO .^{17b} Similar observations apply to the transfer barriers. The transition state of $(\text{H}_3\text{N}-\text{H}-\text{NH}_3)^+$ is higher in energy than the two symmetric wells by 3.9 kcal/mol whereas the left and right wells of $(\text{H}_2\text{CHN}-\text{H}-\text{NH}_3)^+$ are respectively 5.9 and 3.1 kcal/mol lower in energy than the transition state. (The energy surfaces of the oxygen analogues $(\text{H}_2\text{O}-\text{H}-\text{OH}_2)^+$ and $(\text{H}_2\text{CO}-\text{H}-\text{OH}_2)^+$ each contain a single minimum.)

We have not included zero-point vibrational energies in the above discussion as we are concerned primarily with intrinsic electronic effects. While the dissociation energies would be altered in absolute magnitude by vibrational contributions, the bracketing trend is expected to be unaffected and has in fact been confirmed by experimental data.²⁶ Moreover, previous work has demonstrated that inclusion of zero-point vibrations has very little effect on the energy barriers.^{17b}

The H bond length $R(\text{NN})$ is 2.823 Å in the $(\text{H}_2\text{CHNH}-\text{NH}_3)^+$ complex. This length contracts by 0.24 Å in the transition state and then elongates to 2.788 Å at the completion of the proton transfer. Similar trends were noted in $(\text{H}_3\text{N}-\text{H}-\text{NH}_3)^+$ where $R(\text{NN})$ is reduced by 0.20 Å, from 2.797 Å in $(\text{H}_3\text{NH}-\text{NH}_3)^+$ to 2.599 Å in $(\text{H}_3\text{N}-\text{H}-\text{NH}_3)^+$. This shortening of the H bond in the transition state has been noted previously in a number of other systems.⁹⁻¹⁷ The central proton stays essentially along the N-N axis throughout the transfer, varying by less than 1° from this line at any point.

The CN-N angle α undergoes a small increase from 122° to 129° as the transfer progresses whereas β decreases slightly. The initial value of +2.3° for β is probably due to the fact that the positive charge of the $(\text{H}_2\text{CNH}_2)^+$ subunit is not evenly distributed above and below the N-N axis. The CH_2 group is more highly charged than is H_N as revealed by Mulliken charges of 0.68 and 0.47, respectively. Hence, the dipole moment of NH_3 , oriented along its C_3 axis, is somewhat more attracted to the CH_2 group and a slightly positive β results. This factor becomes less important as the proton approaches NH_3 and β is consequently diminished. The $\theta(\text{CNH})$ angle in $(\text{H}_2\text{CNH}_2)^+$ is 122°, as indicated in the first row of Table I. It is therefore not surprising that α adopts a similar value in $(\text{H}_2\text{CHNH}-\text{NH}_3)^+$ so as to allow H^c to lie along the N-N axis without inducing any strain into the $(\text{H}_2\text{CNH}_2)^+$ subunit. As the proton is transferred across to NH_3 , the angle α tends toward that value that will best allow the lone pair of H_2CNH to interact with the H-bonding proton. Calculations of the isolated H_2CNH molecule indicate the lone pair direction, defined as the maximum of the total electron density, occurs 129° from the C=N bond, explaining the value of α in $(\text{H}_2\text{CHN}-\text{HNH}_3)^+$. A second factor in the larger value of α in the latter configuration is the dipole moment of H_2CNH which is oriented at an angle of 136° with respect to the C=N bond. This dipole will tend to turn toward the positive charge of $(\text{NH}_4)^+$, leading to an increase in α over its initial value of 122°.

In order to maintain a linear H bond in the $\text{AH}-\text{B}$ configuration as well as minimize steric strain within AH , the A subunit is oriented so that a lone pair points approximately toward B. On the other hand, a prime consideration in $\text{A}-\text{HB}$ is alignment of the dipole moment of A with the H bond axis. Since the single lone pairs of both H_2CNH and NH_3 are coincident, or nearly so, with the molecular dipole moment vectors, there is little reorientation of the subunits necessary during proton transfer in $(\text{H}_2\text{CHN}-\text{H}-\text{NH}_3)^+$. In contrast, the oxygen analogues H_2CO and H_2O each contain two lone pairs, both of which deviate from the dipole moment direction of the molecule by a substantial angle. For this reason, the reorientations of the two subunits occurring as a result of proton transfer in $(\text{H}_2\text{CO}-\text{H}-\text{OH}_2)^+$ are much greater, on the order of 30° or more.^{17b}

Variation of H Bond Length

The above calculations are directly applicable to the gas-phase H-bonded complex involving the methylenimine and ammonia molecules. As a second situation, we consider both the imine and amine groups to be located on a single molecule. In this case, the distance between them is determined largely by structural constraints external to the H bond itself. Since these constraints will remain in force throughout the proton-transfer process, it would be more appropriate here to hold the H bond length fixed in our calculations. For each of three values of $R(\text{NN})$, a proton-transfer potential was therefore generated, holding $R(\text{NN})$ constant but allowing all other geometrical parameters to vary. These three $R(\text{NN})$ distances were chosen as 2.55, 2.75, and 2.95 Å for purposes of comparison with the analogous $(\text{H}_2\text{CO}-\text{H}-\text{OH}_2)^+$ system.^{17b} The results are presented in Table II which contains the optimized geometries of the two minima in each potential as well as the maximum separating them. As in the previously described case allowing variation of R along the proton-transfer coordinate, α increases by about 5° as a result of transfer of the proton from H_2CNH to NH_3 and β tends toward 0°.

The energies listed in the last column of Table II are relative to the lowest energy $(\text{H}_2\text{CHNH}-\text{NH}_3)^+$ configuration for each value of R . The energy barrier for proton transfer from imine to amine may be seen to be 2.5 kcal/mol for $R = 2.55$ Å and to climb rapidly as R is increased. This dependence of transfer barrier E^\ddagger upon H bond length is illustrated by the curve labeled $\text{CNH} \rightarrow \text{N}$ in Figure 2. The barriers for transfer in the reverse direction are represented by the other solid curve labeled $\text{CH} \leftarrow \text{HN}$; these reverse barriers are uniformly lower due to the fact that the right well in the potential is higher in energy than the left.

(26) Yamdagni, R.; Kebarle, P. *J. Am. Chem. Soc.* **1973**, *95*, 3504. Davidson, W. R.; Sunner, J.; Kebarle, P. *Ibid.* **1979**, *101*, 1675. Larson, J. W.; McMahon, T. B. *Ibid.* **1982**, *104*, 6255. Caldwell, G.; Rozeboom, M. D.; Kiplinger, J. P.; Bartmess, J. E. *Ibid.* **1984**, *106*, 4660. Bomse, D. S.; Beauchamp, J. L. *J. Phys. Chem.* **1981**, *85*, 488.

Table II. Geometries of $(\text{H}_2\text{CHN}-\text{H}-\text{NH}_3)^+$ During the Transfer Process (All Distances in Å and Angles in deg)

| $r(\text{N}^+\text{H}^c)$ | $r(\text{CN}^a)$ | $r(\text{N}^+\text{H}_\text{N})$ | $r(\text{CH}_1)$ | $r(\text{CH}_2)$ | $r(\text{N}^b\text{H})$ | δ | α | β | $\theta(\text{H}_1\text{CN}^a)$ | $\theta(\text{H}_2\text{CN}^a)$ | $\theta(\text{CN}^+\text{H}_\text{N})$ | $\theta(\text{HN}^b\text{H})$ | E , kcal/mol |
|-----------------------------------|------------------|----------------------------------|------------------|------------------|-------------------------|----------|----------|---------|---------------------------------|---------------------------------|--|-------------------------------|------------------|
| $R(\text{NN}) = 2.55 \text{ \AA}$ | | | | | | | | | | | | | |
| 1.075 | 1.256 | 1.005 | 1.074 | 1.074 | 1.008 | -1.4 | 124.0 | 2.9 | 121.4 | 119.5 | 118.4 | 106.1 | 0.0 ^a |
| 1.308 | 1.254 | 1.006 | 1.076 | 1.076 | 1.009 | -0.5 | 125.2 | 1.4 | 122.4 | 119.7 | 115.5 | 107.5 | 2.5 |
| 1.448 | 1.254 | 1.006 | 1.077 | 1.077 | 1.010 | -0.9 | 128.5 | 1.2 | 123.0 | 119.8 | 113.5 | 108.2 | 1.8 |
| $R(\text{NN}) = 2.75 \text{ \AA}$ | | | | | | | | | | | | | |
| 1.052 | 1.256 | 1.004 | 1.074 | 1.074 | 1.006 | 0.3 | 122.3 | 2.2 | 119.5 | 121.0 | 120.0 | 106.1 | 0.0 ^b |
| 1.392 | 1.253 | 1.004 | 1.075 | 1.076 | 1.008 | 0.0 | 122.6 | 0.2 | 119.8 | 122.8 | 116.8 | 108.0 | 8.7 |
| 1.684 | 1.253 | 1.006 | 1.078 | 1.077 | 1.010 | -0.6 | 129.2 | 0.9 | 123.2 | 119.9 | 112.7 | 108.8 | 2.7 |
| $R(\text{NN}) = 2.95 \text{ \AA}$ | | | | | | | | | | | | | |
| 1.041 | 1.257 | 1.004 | 1.074 | 1.074 | 1.005 | 0.3 | 122.1 | 2.3 | 120.6 | 119.4 | 120.7 | 106.2 | 0.0 ^c |
| 1.486 | 1.253 | 1.004 | 1.076 | 1.075 | 1.007 | -0.3 | 125.2 | 0.9 | 122.0 | 120.0 | 116.7 | 108.5 | 17.3 |
| 1.899 | 1.253 | 1.006 | 1.079 | 1.077 | 1.011 | -0.4 | 129.8 | 0.7 | 123.4 | 119.9 | 112.3 | 109.2 | 3.2 |

^a $E^{\text{SCF}} = -150.45540$ au. ^b $E^{\text{SCF}} = -150.46074$ au. ^c $E^{\text{SCF}} = -150.46029$ au.

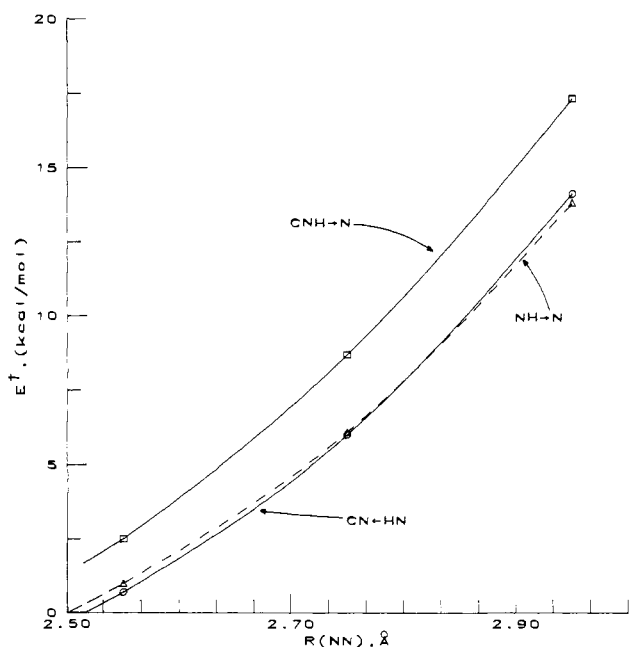


Figure 2. Dependence of proton-transfer energy barrier E^\ddagger upon the length of the H bond. Transfer from imine to amine in $(\text{H}_2\text{CHN}-\text{H}-\text{NH}_3)^+$ is denoted $\text{CNH}\rightarrow\text{N}$; $\text{CN}\leftarrow\text{HN}$ refers to the reverse direction of transfer. The broken curve corresponds to the $(\text{H}_3\text{N}-\text{H}-\text{NH}_3)^+$ system.

For purposes of comparison, proton-transfer potentials were also calculated for identical $R(\text{NN})$ distances in the $(\text{H}_3\text{N}-\text{H}-\text{NH}_3)^+$ system. The computed barriers are illustrated by the broken curve labeled $\text{NH}\rightarrow\text{N}$ in Figure 2. Let us take as a starting point the symmetric proton-transfer potential for this system, designated $\text{AH}\rightarrow\text{A}$, and consider perturbations introduced by replacement of the left-hand A subunit by a group B of higher proton affinity. One would expect that as the proton moves toward this subunit, the system would be progressively stabilized. That is, $\text{B}\rightarrow\text{HA}$ is stabilized the least, $\text{B}\rightarrow\text{H}\rightarrow\text{A}$ by a larger amount, and $\text{BH}\rightarrow\text{A}$ the most.⁹ It is therefore not surprising that replacement of the left H_3N of $(\text{H}_3\text{N}-\text{H}-\text{NH}_3)^+$ by the more basic H_2CNH raises the left \rightarrow right transfer barrier, as indicated by a comparison of the $\text{NH}\rightarrow\text{N}$ and $\text{CNH}\rightarrow\text{N}$ curves in Figure 2.

Although the above replacement would lead us to expect a lowered barrier for transfer from right to left, we find instead that the $\text{CN}\leftarrow\text{HN}$ curve in Figure 2 is nearly coincident with the $\text{NH}\rightarrow\text{N}$ data. This similarity is due to a second and opposing effect which acts to raise the former barrier and arises from a difference in the equilibrium $r(\text{NH})$ bond lengths in the isolated $(\text{NH}_4)^+$ and $(\text{H}_2\text{CNH}_2)^+$ subunits which are 1.014 and 1.006 Å, respectively. Since we are considering fixed and equal N-N separations in $(\text{H}_3\text{N}-\text{H}-\text{NH}_3)^+$ and $(\text{H}_2\text{CHNH}-\text{H}-\text{NH}_3)^+$, the proton has a further distance to move between the two N atoms (the two equilibrium positions of the proton are further apart) in the latter

system due to the shorter $r(\text{NH})$ bond in $(\text{H}_2\text{CNH}_2)^+$. This longer "transfer distance" leads to a higher transfer barrier in the same manner as does a lengthening of the H bond distance $R(\text{NN})$.^{9,13} A similar, albeit smaller, difference in $r(\text{OH})$ between $(\text{H}_2\text{COH})^+$ and $(\text{H}_3\text{O})^+$ is responsible for nearly equal $\text{OH}\rightarrow\text{O}$ and $\text{CO}\leftarrow\text{HO}$ transfer barriers in $(\text{H}_2\text{O}-\text{H}-\text{OH}_2)^+$ and $(\text{H}_2\text{CO}-\text{H}-\text{OH}_2)^+$, respectively.^{17b}

The increase of barrier height associated with elongation of the H bond continues beyond the limit of $R = 2.95 \text{ \AA}$ used to draw Figure 2. For example, the $\text{CNH}\rightarrow\text{N}$ and $\text{CN}\leftarrow\text{HN}$ barriers for $R = 3.2 \text{ \AA}$ were calculated to be 30.2 and 27.0 kcal/mol, respectively. Due to its sensitivity to barrier height,¹⁴ the rate of transfer would be drastically reduced by stretches of the H bond. In contrast to the rapid increase in E^\ddagger , the parallel nature of the curves in Table II indicates an approximately constant value of ΔE , the difference in energy between the $(\text{H}_2\text{CHNH}-\text{H}-\text{NH}_3)^+$ and $(\text{H}_2\text{CHN}-\text{H}-\text{NH}_3)^+$ configurations, in agreement with results for other systems including $(\text{H}_2\text{CO}-\text{H}-\text{OH}_2)^+$. In fact, ΔE does vary slightly with R , particularly for short H bonds. For example, ΔE increases from 1.9 kcal/mol for $R = 2.55 \text{ \AA}$ to 3.1 for $R = 2.95 \text{ \AA}$ whereas a further stretch to 3.2 \AA is associated with an additional increment of only 0.2 kcal/mol. Another point concerns the intercept of the curves in Figure 2 with the horizontal axis. We see that the barrier for $\text{CN}\leftarrow\text{HN}$ transfer vanishes when $R(\text{NN})$ is reduced to 2.51 \AA at which point the potential collapses into a single-well function. It is interesting that this transition from double- to single-well character occurs at almost precisely the same H bond length in $(\text{H}_2\text{CO}-\text{H}-\text{OH}_2)^+$.

Previous work has suggested that for certain systems, proton-transfer energetics, calculated as described above, may be approximated to good accuracy with the "rigid molecule" approximation wherein the coordinates of all atoms are held fixed as the proton is shifted along the H bond axis.⁹⁻¹³ Calculations using this approach reproduced the data in Figure 2 with the following systematic deviations. The $\text{CNH}\rightarrow\text{N}$ barriers were exaggerated by about 0.7 kcal/mol while the barriers for the reverse transfer were underestimated by between 0.6 and 1.5 kcal/mol. In order to understand these results, it must be remembered that the rigid molecule approximation uses the geometry of the left well, i.e., $(\text{H}_2\text{CHNH}-\text{H}-\text{NH}_3)^+$ configuration, throughout the entire proton transfer. Motion of the proton toward NH_3 hence leads to a progressively poorer approximation of the "true" or optimized geometry and therefore to a larger positive deviation of the energy from the true potential. The overestimated energy of the $(\text{H}_2\text{CHN}-\text{H}-\text{NH}_3)^+$ midpoint thus leads to an exaggerated $\text{CNH}\rightarrow\text{N}$ barrier; the reverse barrier is underestimated since the $(\text{H}_2\text{CHN}-\text{H}-\text{NH}_3)^+$ geometry is more in error than is the midpoint. Use of the rigid molecule approximation might therefore save a great deal of computational effort, provided one is aware of the errors involved and correction is made for them.

Angular Dependence

In addition to preventing the H bond from attaining its optimal length, the structural constraints imposed on an intramolecular

Table III. Energetics (in kcal/mol) for Angular Distortions Involving Left Subunit; $R(\text{NN}) = 2.75 \text{ \AA}$

| | $(\text{H}_2\text{CHN-H-NH}_3)^+$ | $(\text{H}_3\text{N-H-NH}_3)^+$ |
|--|-----------------------------------|---------------------------------|
| $\chi, \text{ deg}$ | 51 | 51 |
| $\Delta E(0^\circ)^b$ | 2.5 | 0.0 |
| $\Delta E(\chi)$ | 4.8 | 2.6 |
| $\Delta E(\chi) - \Delta E(0^\circ)$ | 2.3 | 2.6 |
| $\delta E(\text{NH--N})^c$ | 7.4 | 7.8 |
| $\delta E(\text{N--HN})$ | 9.7 | 10.4 |
| $E^\ddagger(0^\circ)^d$ | 8.5 | 6.1 |
| $E^\ddagger(\chi)$ | 22.8 | 20.0 |
| $E^\ddagger(\chi) - E^\ddagger(0^\circ)$ | 14.3 | 13.9 |

^a χ measures deviation from optimized geometry: $\chi = \alpha - 129^\circ$ in $(\text{H}_2\text{CHN-H-NH}_3)^+$ and is equal to the angle between the N--N axis and the C_3 symmetry axis of H_3N in $(\text{H}_3\text{N-H-NH}_3)^+$. ^b $\Delta E = E(\text{N--HN}) - E(\text{NH--N})$. ^c $\delta E = E(\chi) - E(0^\circ)$. ^d $E^\ddagger = E(\text{N--H--N}) - E(\text{NH--N})$.

H bond would be expected to include angular restrictions as well. Indeed, nonlinear H bonds are the rule rather than the exception in a large array of biological macromolecules.²⁷ We model this situation in our calculations by calculating proton-transfer potentials for a series of fixed intermolecular orientation angles.

We begin with an examination of the effects of bending the H_2CNH subunit relative to the N--N axis with the H bond length $R(\text{NN})$ held at a fixed value of 2.75 \AA . For this distance, the optimized value of α in the $(\text{H}_2\text{CHN--HNH}_3)^+$ configuration is 129° , as may be seen in Table II. We therefore consider this geometry as containing no angular distortions and assign a value of 0° to a "distortion angle" χ , defined as $\alpha - 129^\circ$. As mentioned above, ΔE is the difference in energy between the two minima in each transfer potential: $\Delta E = E(\text{N--HN}) - E(\text{NH--N})$. The first value of $\Delta E(0^\circ)$ in Table III thus indicates that the $(\text{H}_2\text{CHN--HNH}_3)^+$ configuration is 2.5 kcal/mol higher in energy than $(\text{H}_2\text{CHNH--NH}_3)^+$ in the undistorted system. The symmetry of $(\text{H}_3\text{N-H-NH}_3)^+$ leads to identical energies for $(\text{H}_3\text{NH--NH}_3)^+$ and $(\text{H}_3\text{N--HNH}_3)^+$ and hence to a zero value of ΔE , as displayed in the last column of Table III.

We now introduce an angular distortion into both systems as follows. The H_2CNH subunit was rotated such that the C=N bond is coincident with the N--N axis, i.e., $\alpha = 180^\circ$ (or $\chi = 51^\circ$). A distortion of like amount was introduced into $(\text{H}_3\text{N-H-NH}_3)^+$ by bending the C_3 axis of the left-hand H_3N subunit away from the N--N axis by 51° . Despite these deformations, the H bonds remain strong; dissociation to isolated subunits requires nearly 20 kcal/mol. Once the values of χ (51°) and R (2.75 \AA) have been fixed, the proton is allowed to follow its lowest energy path between the two N atoms and all other geometrical parameters are fully optimized for each proton position.

As may be seen in the third row of Table III, ΔE in the angularly distorted $(\text{H}_2\text{CHN-H-NH}_3)^+$ system is 4.8 kcal/mol, representing an increase of 2.3 compared to the undistorted system; the increase in $(\text{H}_3\text{N-H-NH}_3)^+$ is of similar magnitude. This result can be analyzed in some detail by comparing the destabilization energies δE introduced into the various configurations by the 51° angular distortion. As may be seen in the fifth and sixth row of Table III, the energies of the NH--N configurations, $(\text{H}_2\text{CHNH--NH}_3)^+$ and $(\text{H}_3\text{NH--NH}_3)^+$, are raised by 7.4 and 7.8 kcal/mol, respectively, while larger distortion energies are noted for the N--HN configurations.

The above trends may be explained if we consider the electrostatic component of the interaction between the two subunits. Since one subunit is protonated and the other neutral, the electrostatic energy will be dominated by the charge-dipole interaction. In the undistorted NH--N configuration, the left subunit is positively charged with the dipole moment of the right (neutral) subunit pointing toward it. Rotation of the left subunit moves its center of charge very little. Hence, the dipole moment of the

Table IV. Energetics (in kcal/mol) for Angular Distortions Involving Right Subunit; $R(\text{NN}) = 2.75 \text{ \AA}$ and $\chi = 0^\circ$ ^a

| | $(\text{H}_2\text{CHN-H-NH}_3)^+$ | $(\text{H}_3\text{N-H-NH}_3)^+$ | |
|---|-----------------------------------|---------------------------------|------|
| $\beta, \text{ deg}$ | 55 | -55 | 55 |
| $\Delta E(\beta)^b$ | -2.5 | -7.1 | -8.2 |
| $\Delta E(\beta) - \Delta E(0^\circ)$ | -5.0 | -9.6 | -8.2 |
| $\delta E(\text{NH--N})^c$ | 13.4 | 18.0 | 16.8 |
| $\delta E(\text{N--HN})$ | 8.4 | 8.4 | 8.6 |
| $E^\ddagger(\beta)^d$ | 20.9 | 19.0 | 16.2 |
| $E^\ddagger(\beta) - E^\ddagger(0^\circ)$ | 12.4 | 10.5 | 10.1 |

^a $\alpha = 129^\circ$ for $(\text{H}_2\text{CHN-H-NH}_3)^+$ and the C_3 axis of the left H_3N subunit is coincident with the N--N axis in $(\text{H}_3\text{N-H-NH}_3)^+$. ^b $\Delta E = E(\text{N--HN}) - E(\text{NH--N})$. ^c $\delta E = E(\beta) - E(0^\circ)$. ^d $E^\ddagger = E(\text{N--H--N}) - E(\text{NH--N})$.

other subunit continues to point toward the charge of the left throughout the rotation and there is consequently very little effect on the electrostatic energy. In contrast, the left subunit is neutral in the N--HN configuration with its dipole moment pointing toward the positive charge of the other subunit. Rotation of the left subunit turns its dipole moment away from the positive charge of the right subunit, leading to a substantial increase in energy. Thus, the larger magnitude of $\delta E(\text{N--HN})$ than of $\delta E(\text{NH--N})$ can be attributed to an electrostatic destabilization in the former which is not present in the latter.

Prior to introduction of the distortion into the system, the energy barrier E^\ddagger for transfer of the proton from left to right is 8.5 kcal/mol for $(\text{H}_2\text{CHN-H-NH}_3)^+$ and 6.1 kcal/mol for $(\text{H}_3\text{N-H-NH}_3)^+$, as listed in the seventh row of Table III. The succeeding rows show that rotation of the left-hand subunit by 51° produces a marked increase in each of these barriers, in conformity with previous calculations linking generally higher transfer barriers to misalignments of the subunits.⁹⁻¹³

Let us now consider the case where the right subunit is rotated. As in the previous case, we hold $R(\text{NN})$ fixed at 2.75 \AA . We also restrict the left subunit to maintain a fixed orientation with respect to the H bond. Specifically, the left subunit is held in its optimal $\chi = 0^\circ$ alignment. The right NH_3 subunit was rotated by setting β equal to half the tetrahedral angle, 55° . This value has the virtue also of being rather close to the distortion angle of 51° used in our prior examination of the rotation of the left subunit and will thus facilitate comparison between these two types of distortion. A positive value of β turns the lone pair of the NH_3 subunit up toward the CH_2 group of the imine while it is rotated down toward the H_N atom for negative values. Due to the symmetry of the $(\text{H}_3\text{N-H-NH}_3)^+$ system, positive and negative values of β lead to nearly identical results.

The data reported in Table IV demonstrate that rotation of the right subunit leads to negative values of ΔE , in contrast to the positive quantities observed in the undistorted system or when the left subunit is misaligned (Table III). Thus, rotation of the right subunit shifts the proton equilibrium position from left to right. It is interesting that the downward rotation of the NH_3 subunit in $(\text{H}_2\text{CHN-H-NH}_3)^+$ produces a substantially more negative ΔE than does the $+55^\circ$ misalignment. The third row of Table IV contains the change in ΔE caused by the rotation of the NH_3 subunit from which it is apparent that this perturbation is twice as large for $\beta = -55^\circ$ than for the positive distortion angle in $(\text{H}_2\text{CHN-H-NH}_3)^+$; the change in ΔE is intermediate between these two extremes for $(\text{H}_3\text{N-H-NH}_3)^+$.

The distortion energies of the individual configurations again provide a useful framework for understanding these phenomena. Comparison of the fourth and fifth rows of Table IV points out the greater destabilization of the NH--N configuration than of N--HN caused by the rotation of the right subunit. This trend conforms to our earlier principles involving misalignment of the charge and dipole of the two subunits. That is, rotation of the right-hand NH_3 subunit in the NH--N configuration turns its dipole away from the charged left subunit, leading to a large value of $\delta E(\text{NH--N})$. The distortion energy of the N--HN configuration is much smaller since the alignment of the left dipole with

(27) Schulz, G. E.; Schirmer, R. H. "Principles of Protein Structure"; Springer-Verlag: New York, 1979. Vinogradov, S. N. In "Molecular Interactions"; Ratajczak, H., Orville-Thomas, W. J., Eds.; Wiley: New York, 1981; Vol. 2, pp 179-229.

Table V. Effects of Out-of-Plane Distortions on Energetics of Proton Transfer (kcal/mol); $R = 2.75 \text{ \AA}$

| | $(\text{H}_2\text{CHN-H-NH}_3)^+$ | | $(\text{H}_3\text{N-H-NH}_3)^+$ | |
|--|-----------------------------------|------|---------------------------------|------|
| ϕ , deg | 20 | 40 | 20 | 40 |
| $\Delta E(\phi)^a$ | 2.1 | 1.1 | -0.1 | 0.5 |
| $\Delta E(\phi) - \Delta E(0^\circ)$ | -0.4 | -1.4 | -0.1 | 0.5 |
| $\delta E(\text{NH--N})^b$ | 1.5 | 5.7 | 1.9 | 6.1 |
| $\delta E(\text{N--HN})$ | 1.1 | 4.3 | 1.7 | 6.6 |
| $E^\ddagger(\phi)^c$ | 8.9 | 10.1 | 7.3 | 13.1 |
| $E^\ddagger(\phi) - E^\ddagger(0^\circ)$ | 0.4 | 1.6 | 1.2 | 7.0 |

^a $\Delta E = E(\text{N--HN}) - E(\text{NH--N})$. ^b $\delta E = E(\phi) - E(0^\circ)$. ^c $E^\ddagger = E(\text{N--H--N}) - E(\text{NH--N})$.

the positively charged species on the right is little affected by the rotation of the latter.

These concepts also add insight into the relative effects of the various distortions. From the fifth row of Table IV, it is clear that neither the nature of the system nor the sign of β has much effect on the energy required to rotate the right $(\text{NH}_4)^+$ subunit in the N--HN configuration. This similarity is not surprising since there is little change caused in the alignment between the charge of $(\text{NH}_4)^+$ and the dipole of the neutral subunit on the left in either system. However, when the proton is associated with the left subunit, the direction of rotation of the NH_3 on the right makes a great deal of difference. Upward rotation turns its dipole moment toward the CH_2 group on which resides a large fraction of the positive charge of $(\text{H}_2\text{CHNH})^+$ whereas the misalignment corresponding to -55° turns the NH_3 dipole toward the H_N atom which is less positively charged. Hence, $\delta E(\text{NH--N})$ is considerably larger for the latter rotation. $\delta E(\text{NH--N})$ is intermediate between these two extremes in the $(\text{H}_3\text{N-H-NH}_3)^+$ system due to the more even distribution of charge in the $(\text{NH}_4)^+$ subunit on the left.

The magnitudes of the energy changes described above for $R(\text{NN}) = 2.75 \text{ \AA}$ are rather large and there is some question as to how these effects might be diminished as the H bond is elongated. Calculations were therefore carried out for $(\text{H}_2\text{CHN-H-NH}_3)^+$ with $R = 3.2 \text{ \AA}$ and the results are as follows. The distortion energy associated with $\beta = -55^\circ$, $\delta E(\text{NH--N})$, is lowered from 18.0 kcal/mol at $R = 2.75 \text{ \AA}$ to 12.0 at $R = 3.2 \text{ \AA}$ and $\delta E(\text{N--HN})$ from 8.4 to 5.6. The net effect is that ΔE is decreased by 6.4 kcal/mol from 3.3 to -3.1 when $R = 3.2 \text{ \AA}$, which compares with a lowering of 9.6 for $R = 2.75 \text{ \AA}$. Thus, the 0.45 \AA stretch of the H bond leads to a general reduction of the energetic effects by about $1/3$. Nevertheless, even for this rather long H bond of 3.2 \AA , the sign of ΔE is reversed by the misalignment of the NH_3 subunit.

Out-of-Plane Distortions. The previous misalignments have involved rotations of the two subunits around axes perpendicular to the H_2CNH molecular plane and have consequently allowed the lone pairs of both subunits to remain in this plane. We now turn our attention to angular distortions which take the NH_3 subunit out of the plane of H_2CNH as follows. The "undistorted" geometry with $\alpha = 129^\circ$ was taken as a starting point, and the NH_3 subunit was then rotated directly up out of the plane of the paper of Figure 1 by an angle ϕ , keeping R fixed at 2.75 \AA . Since the local C_{3v} symmetry of the H_3N molecule does not lead to a unique "molecular plane", the out-of-plane angle ϕ in $(\text{H}_3\text{N-H-NH}_3)^+$ is identical with the χ angle defined in a previous section.

From our previous discussions, we would expect that these misalignments, which move the right subunit away from the dipole moment of the left, would preferentially destabilize the N--HN configuration and lead to an increase in ΔE . This is in fact observed in the case of $(\text{H}_3\text{N-H-NH}_3)^+$ for distortions of greater than 20° , as shown in Table V. In contrast to this expectation, however, the out-of-plane distortions in the $(\text{H}_2\text{CHN-H-NH}_3)^+$ case lead to significant *decreases* in ΔE . The distortion energies in the succeeding rows provide an explanation of this seemingly anomalous behavior. Motion of the NH_3 subunit raises the energy of the NH--N configuration of both systems by approximately equal amounts. However, the distortion energies of the N--HN

configuration are of considerably smaller magnitude for $(\text{H}_2\text{CHN-H-NH}_3)^+$.

The distinction arises from consideration of the quadrupole moments of the H_2CNH and H_3N subunits. The components of the H_3N quadrupole are positive in both directions perpendicular to its C_3 axis or "lone pair direction". Hence, rotation of the right-hand cationic species off the C_3 axis leads to an additional destabilization from the quadrupole-charge interaction. In contrast, the out-of-plane component of the H_2CHN quadrupole moment is negative. Thus, the quadrupole-charge interaction is stabilizing for the out-of-plane motion and the total electrostatic contribution to the distortion energy is therefore less positive. The last two rows of Table V highlight another important difference between the $(\text{H}_2\text{CHN-H-NH}_3)^+$ and $(\text{H}_3\text{N-H-NH}_3)^+$ systems. Although out-of-plane distortions raise the energy barriers for proton transfer, this increase is several times smaller in the former case. This discrepancy may again be attributed to the negative out-of-plane component of the H_2CHN quadrupole moment which may favorably interact with the partial positive charge of the proton in the "distorted" transition state. This distinction between the planar imine and pyramidal amine groups appears to be a general one as previous calculations found much smaller barrier increases in $(\text{H}_2\text{CO-H-OH}_2)^+$ with an sp^2 planar arrangement about the carbonyl oxygen than in $(\text{H}_2\text{O-H-OH}_2)^+$ where the hydroxyl O is hybridized in a pyramidal sp^3 fashion.^{17b}

Summary and Discussion

The fully optimized structure of $(\text{H}_2\text{CHNH--NH}_3)^+$ contains a linear H bond with the proton more closely associated with the imine subunit. This complex is stable by 24.5 kcal/mol with respect to the isolated $(\text{H}_2\text{CNH}_2)^+$ and NH_3 subunits. A second minimum corresponding to $(\text{H}_2\text{CHN--H-NH}_3)^+$ is present in the surface and is 2.8 kcal/mol higher in energy. The transition state to proton transfer between these two minima involves a 0.24- \AA contraction of the N--N H bond length and is 5.9 kcal/mol higher in energy than the lower of the two minima. The surface of $(\text{H}_3\text{N-H-NH}_3)^+$ is quantitatively quite similar except that the two minima are symmetrically equivalent.

Elongation of the H bond leads to an increase in the proton transfer energy barriers in both systems. The barriers for imine \rightarrow amine transfer in $(\text{H}_2\text{CHN-H-NH}_3)^+$ are uniformly higher by several kcal/mol than the values for the reverse direction. Transfer of a proton from H_3N to either H_2CNH or NH_3 involves nearly identical energy barriers over a range of intermolecular distance. In contrast to E^\ddagger , the difference in energy ΔE between the $(\text{H}_2\text{CHNH--NH}_3)^+$ and $(\text{H}_2\text{CHN--H-NH}_3)^+$ configurations is relatively insensitive to the distance between the subunits. The transfer of a proton between N atoms occurs without substantial reorientation of the two subunits, in contrast to interoxygen transfers where the subunits turn by ca. 30° with respect to one another. This distinction is attributed to the fact that the dipole moment vectors of the O bases do not coincide with the directions of the lone pairs.

In addition to studying the proton-transfer process at fixed H bond lengths, a number of angular constraints are imposed as well in order to model transfers in intramolecular bonds. Rotation of either subunit away from its preferred orientation acts to "pull" the proton toward it, i.e., rotation of subunit A stabilizes the AH--B configuration relative to A--HB. The higher energy of A--HB is due primarily to the misalignment of the dipole moment of A from the positive charge of BH^+ resulting from the rotation of the former group. In the case of $(\text{H}_2\text{CHN-H-NH}_3)^+$ where the imine is intrinsically more basic, rotation of this group reinforces the greater stability of $(\text{H}_2\text{CHNH--NH}_3)^+$ whereas a misalignment of the amine reverses the relative energies with $(\text{H}_2\text{CHN--H-NH}_3)^+$ becoming the more stable.

In contrast to the above patterns for N bases, rotation of the carbonyl subunit of $(\text{H}_2\text{CO-H-OH}_2)^+$ away from its preferred orientation acts to stabilize $(\text{H}_2\text{CO--HOH}_2)^+$ rather than $(\text{H}_2\text{COH--OH}_2)^+$. The undistorted geometry is determined largely by the lone pair direction of the carbonyl group which differs from the dipole moment vector by a substantial amount. Rotation of this group stabilizes the former configuration by

bringing the H_2CO dipole moment in better alignment with the charge of HOH_2^+ .

Examination of the effects of motion of the proton-acceptor group out of the plane of the imine group upon the transfer energetics points out markedly different behavior between the imine and amine. Rather than stabilizing the $\text{NH}-\text{N}$ configuration as is observed in $(\text{H}_3\text{NH}-\text{NH}_3)^+$, this out-of-plane distortion preferentially stabilizes $(\text{H}_2\text{CHN}-\text{HNH}_3)^+$. This apparent anomaly is attributed to the attractive electrostatic interaction between the charge of HNH_3^+ and the negative out-of-plane component of the quadrupole moment of H_2CNH , a feature which acts also to diminish the energy barrier to proton transfer. Very similar distinctions apply to the O analogues carbonyl and hydroxyl.²⁸

With particular regard to the proton transfer energy barriers, in-plane distortions of N bases lead to drastic increases, in contrast

(28) The results for the carbonyl and imine are essentially identical if the out-of-plane angle ϕ is defined relative to the lone pairs of these groups. However, if ϕ is defined relative to the $\text{C}=\text{O}$ axis of the carbonyl, out-of-plane distortion leads to a small increase in ΔE , due to the nonlinearity of the H bond in the $(\text{H}_2\text{COH}-\text{OH}_2)^+$ configuration prior to the distortion.

to the O bases where small reductions are observed. In the case of out-of-plane distortions, the primary factor is the hybridization of the proton-donor molecule: the barrier increases observed for the sp^2 planar carbonyl and imine groups are several times smaller than for the hydroxyl and amine groups with their pyramidal sp^3 structure.

We have elucidated here a number of general rules concerning the proton-transfer reaction. These rules may provide insights into a number of poorly understood chemical and biological processes. For example, it is clear from the concepts developed here that the deprotonation of the imine group of the bacteriorhodopsin Schiff base could be greatly facilitated if the proton-accepting group were positioned along the direction of the N lone pair but was turned so that its own dipole moment was pointing away from the Schiff base nitrogen. Further stabilization of the deprotonated state of the Schiff base would result from displacement of the proton-accepting group out of the imine plane.

Acknowledgment. This research was supported by the National Institutes of Health (GM29391 and AM01059) and by the Research Corp. Computer time was made available by the SIU Computer Center.

Dynamic Jahn-Teller Effects in CH_4^+ . Location of the Transition Structures for Hydrogen Scrambling and Inversion

M. N. Paddon-Row,^{*†§} D. J. Fox,[†] J. A. Pople,^{*†} K. N. Houk,^{*†} and D. W. Pratt^{*†‡}

Contribution from the Departments of Chemistry, Carnegie-Mellon University, Pittsburgh, Pennsylvania 15213, and the University of Pittsburgh, Pittsburgh, Pennsylvania 15260.

Received June 10, 1985

Abstract: The ground state potential energy surface of CH_4^+ is explored by ab initio molecular orbital theory. In agreement with previous studies, Jahn-Teller distortion of the T_d structure to a C_{2v} structure results in stabilization. Computation of harmonic frequencies for this structure shows CH_2D_2^+ to have lowest zero-point energy with two short CD bonds and two long CH bonds. This provides an interpretation of the recent observation that CH_2D_2^+ has an EPR spectrum characteristic of such a species. Two C_s transition states for interconverting equivalent C_{2v} structures of CH_4^+ (or CD_4^+) with permuted hydrogens are also found. The lower energy transition state has a small activation energy that is low enough (1-3 kcal/mol) to permit tunneling between six of these structures, making the four hydrogens in CH_4^+ (or CD_4^+) equivalent in EPR experiments, as observed. The second transition state requires higher activation (12-15 kcal/mol) and permits inversion of the pseudotetrahedral C_{2v} form and hence interconversion of all twelve equivalent structures. The low energy for this process suggests that homochiral alkane radical cations should racemize at moderately low temperatures.

Nearly 50 years have elapsed since the discovery by Jahn and Teller of their now celebrated theorem demonstrating the intrinsic geometric instability of orbitally degenerate electronic states.¹ Electron paramagnetic resonance (EPR) spectroscopy has played a central role in revealing some of the static and dynamic consequences of this theorem. The first unambiguous experimental evidence for the Jahn-Teller effect (JTE) was derived from an EPR study of Cu^{2+} in a zinc fluorosilicate crystal at different temperatures.² Subsequently, many other systems exhibiting the JTE have been probed with this technique.³ One of the most remarkable recent examples is the work of Knight et al.⁴ on the methane radical cation, CH_4^+ , and its deuterated derivatives, in which electron loss from the triply degenerate t_2 orbital of methane can lead to C_{2v} , D_{2d} , and C_{3v} JT-type distortions.

The EPR spectrum of CH_4^+ , produced by three independent techniques and examined in a neon matrix at 4 K, is an approximately isotropic quintet with $a_{\text{H}} = 54.8$ G and $g_{\text{iso}} = 2.0029$,

suggesting the existence of four magnetically equivalent protons on the EPR time scale. This is consistent with an average D_{2d} geometry for the parent ion. However, the corresponding spectrum of CH_2D_2^+ exhibits a nearly isotropic triplet of quintets with $a_{\text{H}} = 121.7$ G, $a_{\text{D}} = 2.22$ G, and $g_{\text{iso}} = 2.0029$. Multiplication of the D hyperfine splitting (hfs) by the appropriate nuclear g -factor ratio yields a corresponding proton hfs of $a_{\text{H}} = 14.6$ G, suggesting the existence of two pairs of magnetically inequivalent "protons" in CH_2D_2^+ . This is consistent only with a C_{2v} geometry. Comparison of these hfs with those predicted by ab initio CI spin density calculations⁵ on CH_4^+ confirms the C_{2v} assignment.

(1) Jahn, H. A.; Teller, E., *Phys. Rev.* **1936**, *49*, 874. Jahn, H. A.; Teller, E. *Proc. R. Soc. (London)* **1937**, *A161*, 220.

(2) Bleaney, B.; Ingram, D. J. E. *Proc. Phys. Soc. (London)* **1950**, *A63*, 408. Abragam, A.; Pryce, M. H. L. *Proc. Phys. Soc. (London)* **1950**, *A63*, 409. Bleaney, B.; Bowers, K. D. *Proc. Phys. Soc. (London)* **1952**, *A65*, 667.

(3) Ham, F. S. In "Electron Paramagnetic Resonance"; Geschwind, S., Ed.; Plenum Press: New York, 1972; p 1. See also: Bersuker, I. B. "The Jahn-Teller Effect and Vibronic Interactions in Modern Chemistry"; Plenum Press: New York 1984.

(4) Knight, L. B., Jr.; Steadman, J.; Feller, D.; Davidson, E. R. *J. Am. Chem. Soc.* **1984**, *106*, 3700.

(5) Feller, D.; Davidson, E. R. *J. Chem. Phys.* **1983**, *80*, 1006.

^{*} Carnegie-Mellon University.

[†] University of Pittsburgh.

[§] Present address: Department of Organic Chemistry, The University of New South Wales, Kensington, N.S.W., Australia 2033.

[‡] Fellow of the J. S. Guggenheim Foundation.